Mixing of isoscalar and isovector magnetic dipole excitation modes in ^{206}Pb and ^{208}Pb: Case of electron scattering form factors

M. Schanz* and A. Richter
Institut für Kernphysik, Technische Hochschule Darmstadt, 6100 Darmstadt, Federal Republic of Germany

E. Lipparini
Dipartimento di Fisica, Università di Trento, 38050 Povo (Trento), Italy
(Received 17 April 1987)

Inelastic electron scattering form factors of the $J^\pi=1^+$ states at excitation energies $E_x=5.800$ and 5.846 MeV in ^{206}Pb and ^{208}Pb, respectively, are discussed in terms of a simple model of isoscalar-isovector mixing. It is known that for these states, which are often called loosely "isoscalar" 1^+ states, about half of the transition strength is accounted for by this mixing. It is demonstrated here that the isoscalar-isovector mixing is also crucial for explaining the momentum dependence and the absolute magnitude of the form factor. The relative importance of the convection current contribution to the form factor with respect to the spin one is also studied. Finally, the isovector $M1$ strength distribution in ^{206}Pb between $E_x=6.7$–8.2 MeV derived from high resolution inelastic electron scattering is shown to agree in shape and magnitude with the one measured recently in an experiment with tagged polarized photons.

I. INTRODUCTION

In ^{208}Pb a $J^\pi=1^+$ state is known[1–6] at an excitation energy $E_x=5.846$ MeV which is excited from the $J^\pi=0^+$ ground state through an $M1$ transition with a transition strength[1,4,5] of $B(M1)\uparrow=1.6\pm0.5\ \mu_N^2$. Very recently, a $J^\pi=1^+$ state at an only 48 keV lower excitation energy, i.e, at $E_x=5.800$ MeV, has also been found[7] in ^{206}Pb, the ground state transition strength being $B(M1)\uparrow=1.5\pm0.4\ \mu_N^2$. The closeness of the excitation energy and of the transition strength leaves little doubt that the 1^+ states in both nuclei are of the same structure.

The $J^\pi=1^+$ state in ^{208}Pb—in the past often called loosely "isoscalar" state—was firstly predicted in a Tamm-Dancoff calculation,[8] and more recently it has been studied in the framework of the random phase approximation (RPA) theory.[9–11] In particular, in Ref. 11 the importance of the mixing of isoscalar and isovector $M1$ excitation modes has been pointed out in a simple two state model using an effective separable particle-hole interaction. This calculation has lead to a $J^\pi=1^+$ state at $E_x=5.82$ MeV and a transition strength of $B(M1)\uparrow=1.10\ \mu_N^2$. Note, that about half of this strength is accounted for by the isoscalar-isovector mixing.

It is the main aim of this paper to show that this mixing is also crucial to explain the momentum dependence and the absolute magnitude of the measured $M1$ form factor[5] in ^{208}Pb. The relative importance of the convection current contribution to the form factor with respect to the spin one is also studied. The model is then applied to the $M1$ form factor of the $J^\pi=1^+$ state at $E_x=5.800$ MeV in ^{206}Pb, which has been measured at low momentum transfer in high-resolution inelastic electron scattering at the Darmstadt electron linear accelerator DALINAC. Finally, evidence is presented that the isovector $M1$ strength distribution in ^{206}Pb between $E_x=6.7$ and 8.2 MeV determined recently in an experiment with tagged polarized photons[12] is in agreement in shape and magnitude with the one derived from the present ^{206}Pb(e,e′) experiment.

In Sec. II some brief comments are made on the experimental technique of the ^{206}Pb(e,e′) experiment, the extraction of the cross section, and the multipole identification. The model for the treatment of the $M1$ form factors of the 1^+ states at $E_x=5.846$ and 5.800 MeV in ^{208}Pb and ^{206}Pb, respectively, is introduced in Sec. III. This section also contains a discussion of the results, and includes some remarks on the isovector $M1$ strength distribution at higher excitation energies in ^{206}Pb. Final comments are made in Sec. IV.

II. EXPERIMENT

A. Experimental technique and spectra

The ^{206}Pb(e,e′) measurement was performed at the Darmstadt 70 MeV electron linear accelerator DALINAC using the same technique employed in the ^{208}Pb(e,e′) high-resolution experiment.[4] The target consisted of a 99.77% isotopically enriched ^{206}Pb metal foil (10.65 mg/cm^2) cooled to liquid N_2 temperature. It, furthermore, was moved periodically in the electron beam through a mechanical wobbler such that it withstood beam currents up to about 11 μA without showing signs of deterioration.

Nine spectra were measured at incident energies between $E_0=25$ and 48 MeV, and primarily at a backward scattering angle of $\theta=165°$. A few runs at a more forward angle of $\theta=117°$ were taken in order to discriminate between the longitudinal and transverse nature of the transitions. The spectra spanned the excitation energy range from $E_x=5.0$ to 8.5 MeV and the energy resolution achieved varied between 22 and 41 keV [full width at half

maximum (FWHM)].

Some of the background subtracted experimental spectra are shown in Figs. 1 and 2. Three spectra at $\theta=165°$ covering the excitation energy region from $E_x \approx 5.0$ to 6.5 MeV are displayed in Fig. 1. The rich structure in these spectra provide clearly evidence for the high level density of ^{206}Pb at the investigated excitation energy, but peaks corresponding to low multipolarity transitions from the ground state into excited states are still visible. Noticeable is the excitation of a $J^\pi=2^+$ state at $E_x=6.103$ MeV which has been used for a precise energy calibration of all measured spectra. The $J^\pi=1^+$ state of interest at $E_x=5.800\pm0.005$ MeV is marked with an arrow. It is seen particularly well only in the spectrum at $E_0=25$ MeV. The three spectra of the excitation energy range from $E_x \approx 6.0$ to 8.3 MeV plotted in Fig. 2 reveal an even richer structure than the one at lower energies, and the levels excited overlap. The appearance of pronounced transition strength between $E_x \approx 7$ and 8 MeV at the backward angle $\theta=165°$ and their relative weakness at the more forward angle $\theta=117°$ points to the transverse nature of this strength. One also notices an increase in magnitude of this transverse strength from the $E_0=35$ MeV to the $E_0=25$ MeV spectrum, i.e., an increase with decreasing momentum transfer q, which is the typical form factor behavior of $M1$ transitions.

B. Inelastic cross section calculation

The spectra in the excitation energy range from $E_x=5.0$ to 6.5 MeV have been unfolded using the line shape of the elastic peak. The area under each fitted inelastic peak was then divided by the area under the corresponding elastic peak, and the ratios, after correction for radiation and spectrometer dispersion effects, were multiplied by the theoretically calculated elastic scattering cross section. The latter were computed in distorted-wave Born approximation (DWBA) phase shift analysis using a two-parameter Fermi charge distribution with parameters[13] $c=6.61$ fm and $t=2.40$ fm.

C. Determination of multipolarity and transition strength

The multipolarity and transition strength of each inelastic transition was determined by a comparison of the measured cross section with cross sections calculated in the DWBA as described in detail [for the case of ^{90}Zr(e,e')] in Ref. 14. The necessary transition densities for the form factor computations for the case of $M1$ transitions were taken from the RPA model introduced in the next section, and for transitions of the other multipolarities up to order $\lambda=3$ from predictions for ^{208}Pb of the model of separable interaction.[15] This method of

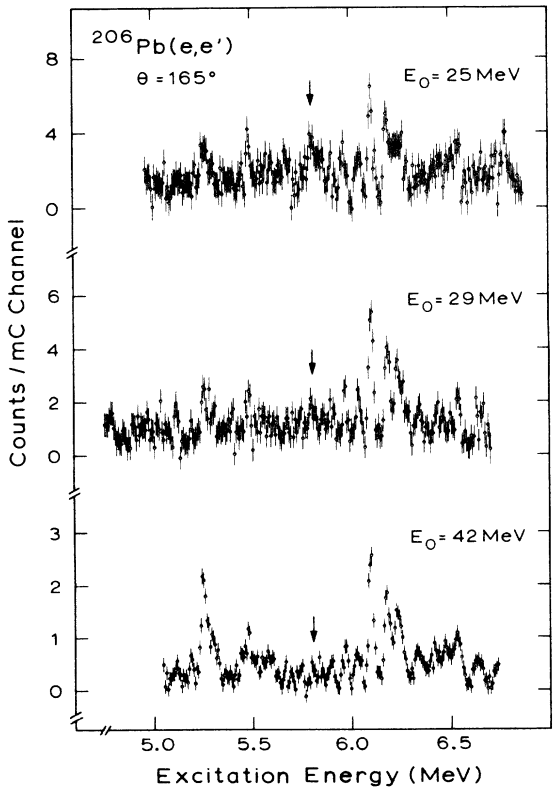

FIG. 1. Background subtracted experimental spectra for ^{206}Pb(e,e') at constant scattering angle $\theta=165°$ but different bombarding energies. The excitation energy ranges from $E_x \approx 5.0$ to 6.5 MeV. The arrow indicates the $J^\pi=1^+$ state at $E_x=5.800$ MeV.

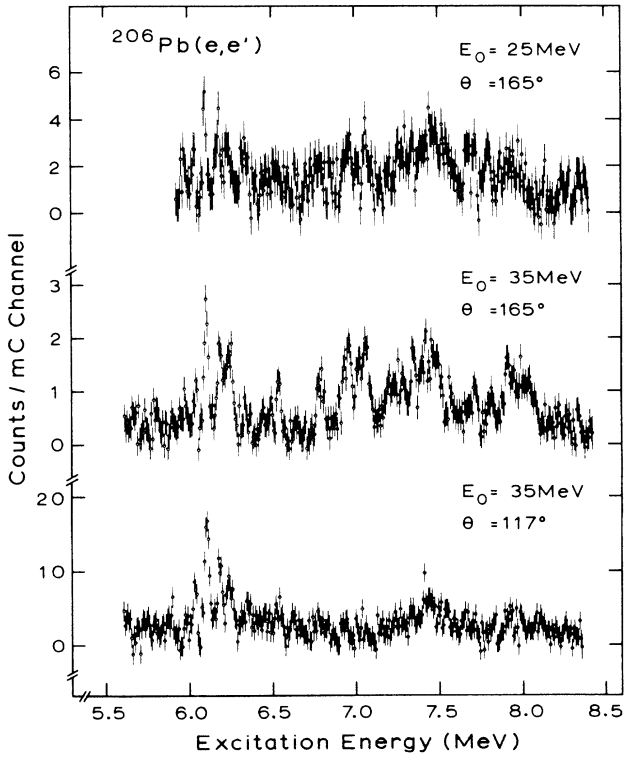

FIG. 2. Background subtracted experimental spectra for ^{206}Pb(e,e') at scattering angles $\theta=117°$ and 165° and two different bombarding energies. The excitation energy ranges from $E_x \approx 6.0$ to 8.3 MeV. The existence of transverse excitation strength between $E_x \approx 7$ and 8 MeV is evident from a comparison between the spectra at the forward and backward angles, respectively.

TABLE I. Levels in ^{206}Pb in the excitation energy range between $E_x = 5.124$ and 6.541 MeV identified in ^{206}Pb(e,e'). Where the spin and parity assignment is uncertain, the less probable assignment is placed second. When a reduced transition strength could be determined it is also given. The uncertainty in the excitation energies is typically between 5 and 10 keV for the stronger transitions and up to 20 keV for the weaker ones.

E_x (MeV)	J^π	$B(X\lambda)$ value	E_x (MeV)	J^π	$B(X\lambda)$ value
5.124	2^+	$38\pm7\ e^2\,\mathrm{fm}^4$	5.760	$1^-,2^+$	
5.261	3^-	$48\,000\pm2000\ e^2\,\mathrm{fm}^6$	5.800	1^+	$1.0\pm0.3\ \mu_N^2$
5.288	$3^-,2^+$		5.846	$1^-,2^+$	
5.309	2^+	$48\pm8\ e^2\,\mathrm{fm}^4$	5.857		
5.448	$2^+,3^-$		5.903	$2^+,1^-$	
5.493	2^+	$38\pm7\ e^2\,\mathrm{fm}^4$	5.969	$2^-,2^+$	
5.564	$1^-,2^+$		6.103	2^+	$185\pm7\ e^2\,\mathrm{fm}^4$
5.480			6.187	2^+	$144\pm7\ e^2\,\mathrm{fm}^4$
5.615	$2^+,1^-$		6.318	$2^+,3^-$	
5.682	$1^-,2^+$		6.347	2^+	$46\pm6\ e^2\,\mathrm{fm}^4$
5.692			6.423	2^+	$38\pm6\ e^2\,\mathrm{fm}^4$
5.715	$1^-,2^+$		6.541	2^-	$292\pm27\ \mu_N^2\,\mathrm{fm}^2$
5.732					

comparison between measured and calculated form factors worked very well for all transitions, except for some weak $E1$ transitions, which are known to show often a noncharacteristic form factor behavior due to the destructive interference of many single particle contributions. Some of the $E1$ excitations in the investigated energy range in ^{206}Pb could, however, be identified with the help of information from photonuclear reactions.[7,16]

The results of this procedure for the lines in the excitation energy range from $E_x \approx 5.0$ to 6.5 MeV are listed in Table I. To many weak excitations an assignment of transition multipolarity has not been possible, and there are also some ambiguous assignments. Most of the observed transitions are of $E1$ and $E2$ nature, except for $E3$ transitions into states at $E_x = 5.261$ and 5.288 MeV. The $J^\pi = 1^+$ state at $E_x = 5.800$ MeV, which we are primarily interested in here, is excited in a transition with a strength of $B(M1)\uparrow = 1.0\pm0.3\ \mu_N^2$.

A decomposition of the spectra in the excitation energy range from $E_x \approx 6.0$ to 8.3 MeV has not easily been possible because of the high level density, the insufficient experimental energy resolution, and the largely overlapping peaks (Fig. 2). All spectra were thus folded such that as they would have been taken with the same energy resolution and divided into energy bins of 50 keV widths. The form factors of the strength in these energy bins have then been compared in a least squares fit to a single form factor and to a combination of two theoretical form factors of different multipolarity. This rather involved procedure, which has been undertaken to obtain the $M1$ strength distribution in the excitation energy range $E_x \approx 6.7$–8.2 MeV by another and independent method from the one of Ref. 12, yielded the results summarized in Table II. Given there are, in each 50 keV wide excitation energy interval ΔE_x (first column), the most likely J^π values of levels excited in this interval (second column) resulting from a fit of a single form factor to the excitation strength observed in this bin, the derived $M1$ strength (third column), the most likely J^π values obtained by fitting the transition strength with a combination of two form factors (fourth column), and the $M1$ strength derived from this approach (fifth column). No listing of values in the fourth column indicates that the cross section in the respective energy bin is already described best by a single form factor.

The multipole decomposition of the experimental transition strength using a combination of two form factors of different multipolarity gives a summed $M1$ transition strength of $\sum B(M1)\uparrow = 14^{+6}_{-9}\ \mu_N^2$ in the excitation energy range $E_x = 6.0$–8.2 MeV. This result is discussed below, but it is interesting to note here that if the total observed (e,e') strength in this energy region would be solely due to $M1$ excitations, one would have 50 μ_N^2, i.e., at most, 28% of the observed strength in the spectra is caused by $M1$ excitations.

III. ISOSCALAR-ISOVECTOR MIXING MODEL AND DISCUSSION

A. Magnetic dipole form factor and transition density

Although the experimental form factors of the $J^\pi = 1^+$ states in ^{208}Pb and ^{206}Pb at $E_x = 5.846$ and 5.800 MeV have been compared to theoretical form factors calculated in the DWBA, for transparency of the procedure the transverse form factor F_T is first introduced in the plane wave Born approximation (PWBA). One has

$$|F_T|^2 = 3\left|\int d\mathbf{r}\, j_1(qr)\mathbf{Y}_{111}(\hat{\mathbf{r}})\cdot\langle 0\,|\,\mathbf{J}(\mathbf{r})\,|\,\omega_{1^+}\rangle\right|^2 , \quad (1)$$

where q denotes the momentum transfer from the electron to the nucleus, $j_1(qr)$ is the spherical Bessel function, $\mathbf{Y}_{111}$ the spherical vector harmonics, and $\mathbf{J}(\mathbf{r})$ the transition current density operator. (Note that the excitation energy of the $J^\pi = 1^+$ state is abbreviated here as ω_{1^+}.) The transition density is the sum of an isoscalar $\mathbf{J}^0(\mathbf{r})$ and an isovector $\mathbf{J}^1(\mathbf{r})$ term,

$$\mathbf{J}(\mathbf{r}) = \mathbf{J}^0(\mathbf{r}) + \mathbf{J}^1(\mathbf{r}) , \quad (2)$$

and (with $\tau^z \mid \mathrm{n}\rangle = \mid \mathrm{n}\rangle$ and $\tau^z \mid \mathrm{p}\rangle = -\mid \mathrm{p}\rangle$)

$$\mathbf{J}^0(\mathbf{r}) = \frac{e}{2m}\left\{(g_{\mathrm{n}}^l + g_{\mathrm{p}}^l)\sum_i \tfrac{1}{2}[\mathbf{p}_i\delta(\mathbf{r}-\mathbf{r}_i) + \delta(\mathbf{r}-\mathbf{r}_i)\mathbf{p}_i] + \frac{1}{2}\frac{g_{\mathrm{n}}^s + g_{\mathrm{p}}^s}{2}\nabla\times\sum_i \boldsymbol{\sigma}_i\delta(\mathbf{r}-\mathbf{r}_i)\right\} \tag{3}$$

and

$$\mathbf{J}^1(\mathbf{r}) = \frac{e}{2m}\left\{(g_{\mathrm{n}}^l - g_{\mathrm{p}}^l)\sum_i \tfrac{1}{2}[\mathbf{p}_i\delta(\mathbf{r}-\mathbf{r}_i) + \delta(\mathbf{r}-\mathbf{r}_i)\mathbf{p}_i] + \frac{1}{2}\frac{g_{\mathrm{n}}^s - g_{\mathrm{p}}^s}{2}\nabla\times\sum_i \boldsymbol{\sigma}_i\delta(\mathbf{r}-\mathbf{r}_i)\right\}\tau_i^z \,. \tag{4}$$

In the two-state model developed in Ref. 11, the RPA transition current densities entering the expression for the form factor are given by

$$\langle 0 \mid \mathbf{J}^0(\mathbf{r}) \mid \omega_{1^+}\rangle = \frac{e}{2m}\left[(g_{\mathrm{n}}^l + g_{\mathrm{p}}^l) + \frac{g_{\mathrm{n}}^s + g_{\mathrm{p}}^s}{4}\left[1 + r\frac{d}{dr}\right]\right] \times f^-(r)\mathbf{r}\times\hat{\mathbf{z}} \tag{5}$$

and

$$\langle 0 \mid \mathbf{J}^1(\mathbf{r}) \mid \omega_{1^+}\rangle = \frac{e}{2m}\left[(g_{\mathrm{n}}^l - g_{\mathrm{p}}^l) + \frac{g_{\mathrm{n}}^s - g_{\mathrm{p}}^s}{4}\left[1 + r\frac{d}{dr}\right]\right] \times f^+(r)\mathbf{r}\times\hat{\mathbf{z}} \tag{6}$$

with

$$f^{\mp}(r) = \frac{3}{16\pi}\left[\frac{1}{2}\left[\left\langle 0\left|\sum_i \sigma_i^z\tau_i^z\right|\omega_{1^+}\right\rangle + \left\langle 0\left|\sum_i \sigma_i^z\right|\omega_{1^+}\right\rangle\right]\frac{R_{l\mathrm{n}}^2(r)}{r^2} \mp \frac{1}{2}\left[\left\langle 0\left|\sum_i \sigma_i^z\tau_i^z\right|\omega_{1^+}\right\rangle - \left\langle 0\left|\sum_i \sigma_i^z\right|\omega_{1^+}\right\rangle\right]\frac{R_{l\mathrm{p}}^2(r)}{r^2}\right] . \tag{7}$$

In Eqs. (3)–(6), e and m denote the proton charge and mass, respectively, and in Eqs. (5) and (6) $\mathbf{r}\times\hat{\mathbf{z}}$ is the vector of Cartesian components $(y, -x, 0)$; $R_{l\mathrm{n}}$ and $R_{l\mathrm{p}}$ are the radial wave functions of the $1i_{13/2}$ neutron and $1h_{11/2}$ proton spin unsaturated shells, respectively. The quantities

$$\left\langle 0\left|\sum_i \sigma_i^z\tau_i^z\right|\omega_{1^+}\right\rangle$$

and

$$\left\langle 0\left|\sum_i \sigma_i^z\right|\omega_{1^+}\right\rangle$$

are the RPA matrix elements of Ref. 11.

Using the results of Eqs. (5)–(7) in evaluating the plane-wave Born approximation (PWBA) form factor of Eq. (1), one finally gets

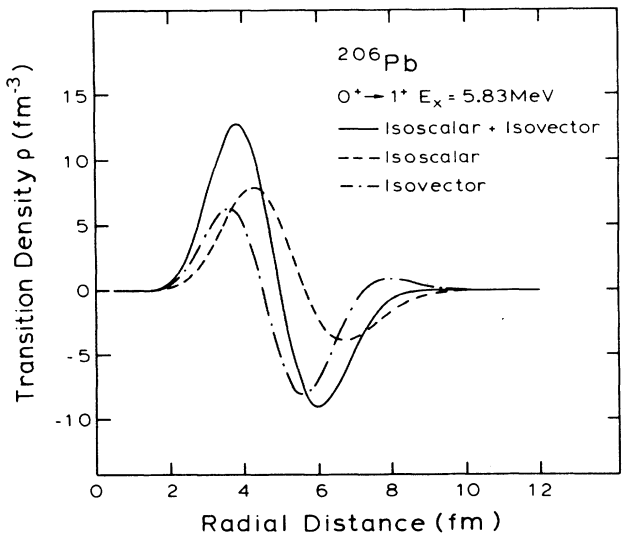

FIG. 3. Isoscalar (dashed line) and isovector (dashed-dotted line) transition current density and the sum of both (solid line) for ^{206}Pb. The excitation energy $E_x = \omega_{1^+} = 5.83$ MeV indicated in the figure is the result of the RPA calculation of Ref. 11.

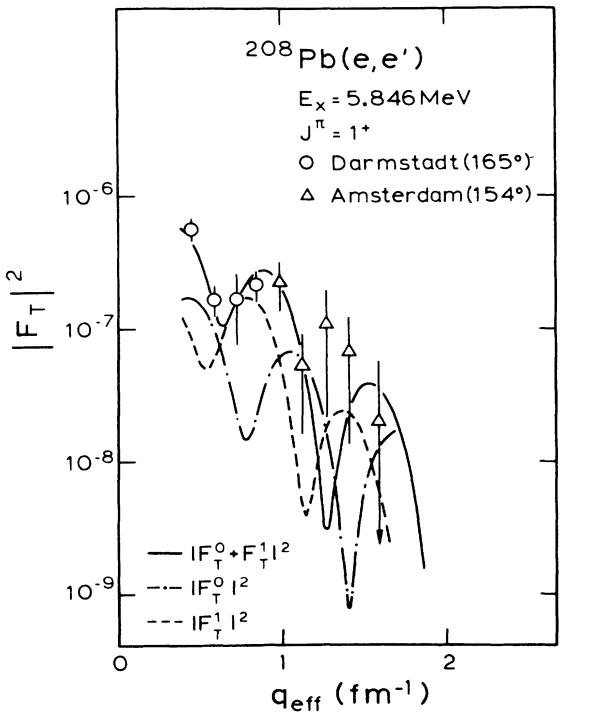

FIG. 4. Comparison of the experimental form factor (Ref. 5) of the $J^\pi = 1^+$ state at $E_x = 5.846$ MeV in ^{208}Pb with the theoretical predictions calculated in the DWBA. The solid line shows the result of the RPA isoscalar-isovector mixing model, while the dashed-dotted and the dashed lines are from the same calculation, assuming a predominant isoscalar and isovector transition current density, respectively.

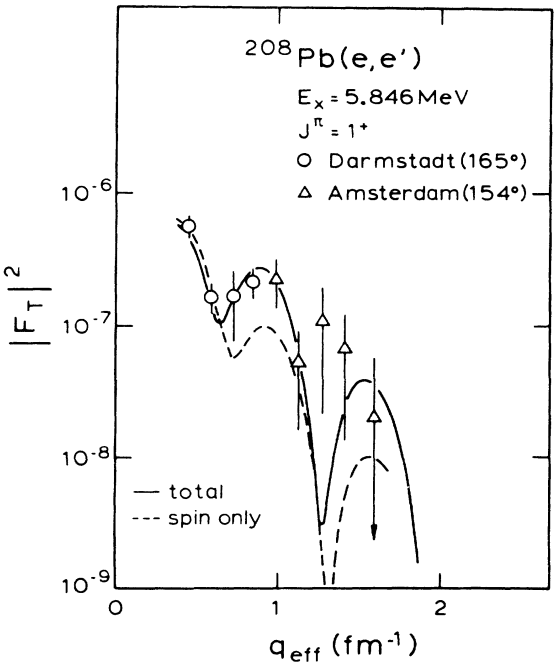

FIG. 5. Comparison of the experimental form factor (Ref. 5) of the $J^\pi = 1^+$ state at $E_x = 5.846$ MeV in ^{208}Pb with the DWBA calculation using the total transition current density (solid line) and with the calculation using only the spin component of the current (dashed line).

$$|F_T|^2 = |F_T^0 + F_T^1|^2 , \tag{8}$$

where

$$F_T^0 = \sqrt{2\pi}\frac{e}{m}\int dr\, r^3 j_1(qr) \times \left[(g_n^l + g_p^l) + \frac{g_n^s + g_p^s}{4}\left[1 + r\frac{d}{dr}\right]\right] f^-(r), \tag{9}$$

$$F_T^1 = \sqrt{2\pi}\frac{e}{m}\int dr\, r^3 j_1(qr) \times \left[(g_n^l - g_p^l) + \frac{g_n^s - g_p^s}{4}\left[1 + r\frac{d}{dr}\right]\right] f^+(r) \tag{10}$$

are the isoscalar and isovector PWBA form factors, respectively.

In the DWBA the cross section still depends on the transition densities given in Eqs. (5) and (6), which contain all the related nuclear structure information. As noted in the introduction to this subsection, the experimental form factors have been compared to form factors calculated in the DWBA, and this comparison is discussed next.

B. Results and discussion

The isoscalar and isovector $M1$ transition densities in ^{206}Pb and ^{208}Pb have been evaluated by using harmonic oscillator radial wave functions for the $1h_{11/2}$ proton and $1i_{13/2}$ neutron orbits (oscillator parameter $b = 2.247$ fm), the free values for the orbital g_l factors, and the values of Ref. 11 for g_n^s, g_p^s, $\langle 0 | \sum_i \sigma_i^z \tau_i^z | \omega_{1^+} \rangle$, and

$$\left\langle 0 \left| \sum_i \sigma_i^z \right| \omega_{1^+} \right\rangle ,$$

yielding a strength $B(M1)\uparrow = 1.04$ and $1.10\ \mu_N^2$ for ^{206}Pb

TABLE II. Results of the multipole decomposition of the experimental transition strength employing one or two multipoles, and the resulting $M1$ transition strength, respectively. No listing of a pair of J^π values means that the experimental form factor is described best by a single theoretical form factor.

ΔE_x (MeV)	J^π	$B(M1)\uparrow$ (μ_N^2)	J^π	$B(M1)\uparrow$ (μ_N^2)
6.00–6.05	1^-		$1^-,2^+$	
6.05–6.10	2^+		$1^+,2^+$	0.4±0.4
6.10–6.15	2^+		$1^-,3^-$	
6.15–6.20	2^+		$1^-,2^+$	
6.20–6.25	2^+		$1^+,3^-$	1.3±0.3
6.25–6.30	1^-		$1^+,3^-$	0.9±0.3
6.30–6.35	1^-			
6.35–6.40	1^-			
6.40–6.45	2^+			
6.45–6.50	1^-		$1^-,3^-$	
6.50–6.55	1^-		$1^+,2^+$	0.6±0.4
6.55–6.60	1^-		$1^-,2^+$	
6.60–6.65	1^-			
6.65–6.70	1^-			
6.70–6.75	1^-			
6.75–6.80	1^-		$1^+,3^-$	1.1±0.3
6.80–6.85	1^-		$1^-,2^-$	
6.85–6.90	1^+	0.9±0.2	$1^+,1^-$	0.8±0.6
6.90–6.95	2^-		$1^-,2^-$	
6.95–7.00	2^-		$1^+,3^+$	1.2±0.4
7.00–7.05	2^-		$1^-,2^-$	
7.05–7.10	2^-		$1^+,3^+$	1.1±0.4
7.10–7.15	1^+	1.0±0.2	$1^+,2^-$	0.7±0.5
7.15–7.20	2^-		$1^-,3^+$	
7.20–7.25	2^-		$1^-,2^-$	
7.25–7.30	1^+	2.0±0.2	$1^-,2^-$	
7.30–7.35	1^+	2.0±0.2	$1^+,3^-$	1.5±0.3
7.35–7.40	2^-		$1^-,2^-$	
7.40–7.45	1^-		$1^-,3^+$	
7.45–7.50	1^+	2.9±0.2	$1^-,2^-$	
7.50–7.55	1^-		$1^+,2^+$	1.3±0.4
7.55–7.60	1^-		$1^+,2^+$	1.0±0.4
7.60–7.65	1^-		$1^+,2^+$	0.6±0.4
7.65–7.70	1^-		$1^+,1^-$	0.4±0.6
7.70–7.75	1^+	1.6±0.2	$1^+,3^-$	1.3±0.3
7.75–7.80	1^+	0.9±0.2	$1^+,1^-$	0.8±0.6
7.80–7.85	1^-		$1^+,3^-$	1.1±0.3
7.85–7.90	1^+	1.2±0.2	$1^+,2^-$	0.8±0.5
7.90–7.95	2^-		$1^-,3^+$	
7.95–8.00	2^-		$1^-,2^-$	
8.00–8.05	2^-		$1^-,3^+$	
8.05–8.10	2^-		$2^+,3^+$	
8.10–8.15	2^+		$1^-,2^+$	
8.15–8.20	2^+		$1^+,3^-$	0.3±0.3
8.20–8.25	2^+		$1^-,3^+$	
8.25–8.30	1^-		$1^-,3^+$	
8.30–8.35	1^-		$1^-,2^-$	

and ^{208}Pb, respectively. Center of mass corrections and the proton finite size corrections have been done in the usual way. Figure 3 shows as an example the isoscalar transition current density (dashed line), the isovector one (dashed-dotted line), and the sum of both (solid line) for ^{206}Pb as a function of radial distance from the center of the nucleus. The isoscalar contribution has its maximum at larger distance than the isovector one, with the result that the minima in the corresponding form factors are also at different places.

The theoretical form factor curves, calculated in the DWBA, for ^{208}Pb, are compared with the data in Fig. 4.[5] Since the experimental points were taken at different scattering angles, the data were plotted as a function of effective momentum transfer[17]

$$q_{\text{eff}} = q\left(1 + \tfrac{4}{3} Z\alpha\hbar c / E_0 A^{1/3}\right) ,$$

where Z and A are the charge and mass number of the target nucleus, respectively, α the fine structure constant, and c the velocity of light. A very good description of the data is achieved in the isoscalar-isovector mixing model (solid line), and the importance of the mixing of the isoscalar and isovector excitations in reproducing both the absolute magnitude of the experimental form factor and its momentum transfer dependence is obvious from the isoscalar (dashed-dotted line) and isovector (dashed line) contributions drawn separately in Fig. 4.

In Fig. 5 the spin current density contribution (dashed line) to the form factor obtained by dropping—in Eqs. (5) and (6)—the terms proportional to g^l is plotted. From the comparison with the total form factor (solid line) one sees that the 1^+ state at 5.846 MeV is indeed mainly a spin excitation.

Finally, the experimental form factor of the $J^\pi = 1^+$ state at $E_x = 5.800$ MeV in ^{206}Pb is compared with the isoscalar-isovector mixing model prediction in Fig. 6. Although the experimental data (mainly the ones from the forward angle measurements) carry sizable error bars, and although the momentum transfer range of the data is limited to low q values, the same holds for what has been discussed in connection with the corresponding form factor in ^{208}Pb.

C. Remarks on the isovector $M1$ strength distribution in ^{206}Pb

It has already been noted in the experimental section that a summed $M1$ transition strength $\sum B(M1)\uparrow = 14^{+6}_{-9}$ μ_N^2 has been found in ^{206}Pb between $E_x \approx 6.0$–8.2 MeV. The distribution of this transition strength in 100 keV energy intervals (open circles) is shown in Fig. 7. Compared to this distribution derived from the (e,e′) experiment is that from a tagged photon experiment[12] (histogram). Considering the much higher sensitivity of the latter experiment and the difficulty of spotting weak $E1$ transitions unambiguously in (e,e′), the agreement between the two distributions is remarkable. The only sizable deviation between the two is seen at $E_x \approx 7.3$ MeV, where the fit of the (e,e′) data with a combined $E1$ and $M2$ form factor gives a slightly better description of the measured strength than a fit with a single $M1$ form factor. The result of the latter fit would have given a strength of about 2 μ_N^2 around $E_x \approx 7.3$ MeV, in better agreement with the results of Ref. 12.

We note in passing that both the center of gravity of the detected $M1$ transition strength between $E_x = 6.7$–8.2 MeV as well as the summed strength itself are in good agreement with the predictions of the RPA model of Ref. 11 for the location and magnitude of the expected isovec-

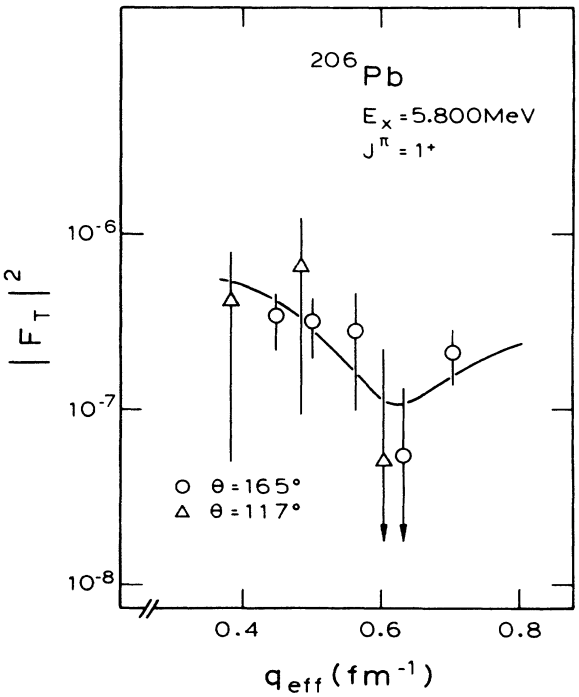

FIG. 6. Comparison of the experimental form factor of the $J^\pi = 1^+$ state at $E_x = 5.800$ MeV in ^{206}Pb with the DWBA calculation using the isoscalar-isovector mixing model.

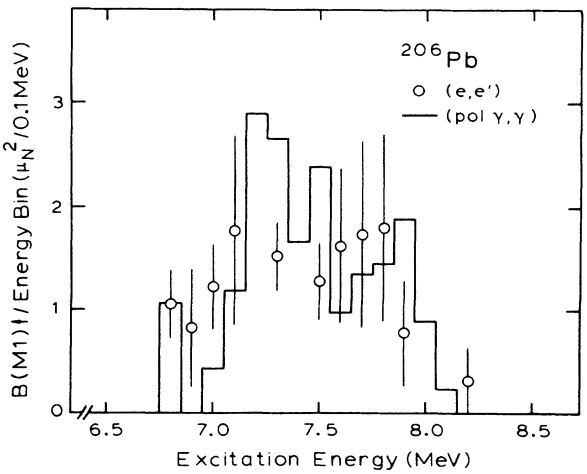

FIG. 7. Comparison of the $M1$ strength per 100 keV wide energy bin from the present ^{206}Pb(e,e′) experiment (open circles) with the $M1$ strength distribution derived from a recent tagged photon experiment (Ref. 12) (histogram).

tor $M1$ strength for the $1h_{11/2}^{-1} \rightarrow 1h_{9/2}$ proton and $1i_{13/2}^{-1} \rightarrow 1i_{11/2}$ neutron spin-flip transitions in the Pb isotopes.

IV. CONCLUSIONS

In spite of the limitations of our model due essentially to the use of an oversimplified particle-hole interaction, we believe that the following findings are rather general:

(1) The mixing of isoscalar and isovector $M1$ transitions is crucial in reproducing the form factor of the $J^{\pi}=1^{+}$ states in ^{206}Pb and ^{208}Pb at low energy.

(2) The transition current density is dominated by the spin component.

We thank G. Kilgus, S. Müller, R. Ratzek, and H. Spangenberger for discussions and help at various stages of this work.

---

*Present address: Leybold-Heraeus GmbH, D-6450 Hanau, Federal Republic of Germany.

[1]K. Wienhard, K. Ackermann, K. Bangert, U. E. P. Berg, C. Bläsing, W. Naatz, A. Ruckelshausen, D. Rück, R. K. M. Schneider, and R. Stock, Phys. Rev. Lett. **49**, 18 (1982).

[2]S. I. Hayakawa, M. Fujiwara, S. Imanishi, Y. Fujita, I. Katayama, S. Morinobu, T. Yamazaki, T. Itahashi, and H. Ikegami, Phys. Rev. Lett. **49**, 1624 (1982).

[3]G. Mairle, K. Schindler, P. Grabmayr, G. J. Wagner, U. Schmidt-Rohr, G. A. P. Berg, W. Hürlimann, S. A. Martin, J. Meissburger, J. G. M. Römer, B. Styczen, and J. L. Tain, Phys. Lett. **121B**, 307 (1983).

[4]S. Müller, A. Richter, E. Spamer, W. Knüpfer, and B. C. Metsch, Phys. Lett. **120B**, 305 (1983); **122B**, 488 (1983).

[5]S. Müller, G. Küchler, A. Richter, H. P. Blok, H. Blok, C. W. de Jager, H. de Vries, and J. Wambach, Phys. Rev. Lett. **54**, 293 (1985).

[6]C. Djalali, J. Phys. (Paris) Colloq. **45**, Suppl. No. 3, C4-375 (1984).

[7]R. Ratzek, U. E. P. Berg, C. Bläsing, A. Jung, S. Schennach, R. Stock, F.-J. Urban, and H. Wickert, Phys. Rev. Lett. **56**, 568 (1986).

[8]J. D. Vergados, Phys. Lett. **36B**, 12 (1971).

[9]J. Wambach, A. D. Jackson, and J. Speth, Nucl. Phys. **A348**, 221 (1980).

[10]S. Drozdz, J. L. Tain, and J. Wambach, Phys. Rev. C **34**, 345 (1986).

[11]E. Lipparini and A. Richter, Phys. Lett. **144B**, 13 (1984).

[12]R. M. Laszewski, P. Rullhusen, S. D. Hoblet, and S. F. LeBrun, Phys. Rev. Lett. **54**, 530 (1985).

[13]C. W. de Jager, H. de Vries, and C. de Vries, At. Data Nucl. Data Tables **14**, 479 (1974).

[14]D. Meuer, R. Frey, D. H. H. Hoffmann, A. Richter, E. Spamer, O. Titze, and W. Knüpfer, Nucl. Phys. **A349**, 309 (1980).

[15]W. Knüpfer and M. G. Huber, Phys. Rev. C **14**, 2254 (1976).

[16]T. Chapuran, R. Vodhanel, and M. K. Brussel, Phys. Rev. C **22**, 1420 (1980).

[17]J. Heisenberg and H. P. Blok, Annu. Rev. Nucl. Part. Sci. **33**, 569 (1983).